Generalized Shock Solutions for Hydrodynamic Black Hole Accretion

Tapas K. Das

Racah Institute of Physics, The Hebrew University of Jerusalem, Israel
IUCAA, Post Bag 4, Ganeshkhind, Pune 411 007, India tapas@iucaa.ernet.in

ABSTRACT

For the first time, *all* available pseudo-Schwarzschild potentials are exhaustively used to investigate the possibility of shock formation in hydrodynamic, invicid, black hole accretion discs. It is shown that a significant region of parameter space spanned by important accretion parameters allows shock formation for flow in *all* potentials used in this work. This leads to the conclusion that the standing shocks are essential ingredients in accretion discs around non-rotating black holes in general. Using a complete general relativistic framework, equations governing multi-transonic black hole accretion and wind are also formulated and solved in the Schwarzschild metric. Shock solutions for accretion flow in various pseudo potentials are then compared with such general relativistic solutions to identify which potential is the best approximation of Schwarzschild space-time as far as the question of shock formation in black hole accretion discs is concerned.

Subject headings: accretion, accretion disks — black hole physics — hydrodynamics — shock waves

---

Published in the The Astrophysical Journal, 2002, Volume 577, Issue 2, pp. 880-892.

---

[1]Present Address: Division of Astronomy, University of California at Los Angeles, Box 951562, Los Angeles, CA 90095-1562, USA; tapas@astro.ucla.edu

1. Introduction

The process by which any gravitating, massive, astrophysical object captures its surrounding fluid is called accretion. Depending on the rotational energy content of the infalling material, accretion flows onto black holes may be broadly classified into two different categories, i.e., non-rotating (spherical) and rotating accretion (accretion discs). If the instantaneous dynamical velocity and local acoustic velocity of the accreting fluid, moving along a space curve parameterized by r, are $u(r)$ and $a(r)$ respectively, then the local Mach number $M(r)$ of the fluid can be defined as $M(r) = \frac{u(r)}{a(r)}$. The flow will be locally subsonic or supersonic according to $M(r) < 1$ or > 1, i.e., according to $u(r) < a(r)$ or $u(r) > a(r)$. The flow is transonic if at any moment it crosses $M = 1$. This happens when a subsonic to supersonic or supersonic to subsonic transition takes place either continuously or discontinuously. The point(s) where such crossing takes place continiously is (are) called sonic point(s), and where such crossing takes place discontinuously are called shocks or discontinuities. It is generally argued that, in order to satisfy the inner boundary conditions imposed by the event horizon, accretion onto black holes exhibit transonic properties in general, which further indicates that formation of shock waves are possible in astrophysical fluid flows onto galactic and extra-galactic black holes. One also expects that shock formation in black hole accretion might be a general phenomena because shock waves in rotating and non-rotating flows are convincingly able to provide an important and efficient mechanism for conversion of significant amount of the gravitational energy (available from deep potential wells created by these massive compact accretors) into radiation by randomizing the directed infall motion of the accreting fluid. Hence shocks possibly play an important role in governing the overall dynamical and radiative processes taking place in accreting plasma. Thus the study of steady, stationary shock waves produced in black hole accretion has acquired a very important status in recent years and it is expected that shocks may be an important ingredient in an accreting black hole system in general.

While the possibility of the formation of a standing spherical shock around compact objects was first conceived long ago (Bisnovatyi-Kogan, Zel'Dovich, & Sunyaev 1971), most of the works on shock formation in spherical accretion share more or less the same philosophy that one should incorporate shock formation to increase the efficiency of directed radial infall in order to explain the high luminosity of AGNs and QSOs and to model their broad band spectrum (Jones & Ellison 1991). Considerable work has been done in this direction where several authors have investigated the formation and dynamics of standing shock in spherical accretion (Mészáros & Ostriker 1983, Protheros & Kazanas 1983, Chang & Osttriker 1985, Kazanas & Ellision 1986, Babul, Ostriker & Mészáros 1989, Park 1990, 1990a). Ideas and formalisms developed in these works have been applied to study related interesting problems like entropic-acoustic or various other instabilities in spherical accretion (Foglizzo & Tagger

2000, Blondin & Ellison 2001, Lai & Goldreich 2000, Foglizzo 2001, Kovalenko & Eremin 1998), production of high energy cosmic rays from AGNs (Protheroe & Szabo 1992), study of the hadronic model of AGNs (Blondin & Konigl 1987, Contopoulos & Kazanas 1995), high energetic emission from relativistic particles in our galactic centre (Markoff, Melia & Sarcevic 1999), explanation of high lithium abundances in the late-type, low-mass companions of the soft X-ray transient, (Guessoum & Kazanas 1999), study of accretion powered spherical winds emanating from galactic and extra galactic black hole environments (Das 2001).

With equal (if not more) importance and rigor, the question of shock formation in accretion discs around Schwarzchild black holes has been addressed by several authors. While the initial works in this direction can be attributed to Fukue (1983), Hawley, Wilson & Smarr (1984), Ferrari et al. (1985), Swada et al. (1986) and Spruit (1987), it was Fukue (1987) and Chakrabarti and his collaborators (Chakrabarti 1989 (C89 hereafter), 1996 and references therein, Abramowicz & Chakrabarti 1990, Chakrabarti & Molteni 1993) who were the first to provide the satisfactory semi-analytical or numerical global shock solution for transonic, invicid, Keplerian or sub-Keplerian rotating accretion around a Schwarzchild black hole. Consequently, their works were further supported and improved by several other independent works (Yang & Kafatos 1995 (YK hereafter), Caditz & Tsuruta 1998, Tóth, Keppens & Botchev 1998). Because of the inner boundary conditions imposed by the event horizon, shocks form in BH accretion discs only if the flow has more than one real physical X type sonic point (multi-transonic flow). For a particular set of initial boundary conditions, some of the above mentioned works report multiplicity in shock location, but such a degeneracy can ultimately be removed by local stability analysis, allowing one to assert that only one stable shock location is possible. Hereafter, whenever we will use the word 'shock', it is to be understood that we will, in general, always refer only the stable shock location unless otherwise mentioned.

The above mentioned works deserve attention because the shocked flows studied there are expected to explain the spectral properties of BH candidates. However, thus far in the astrophysical literature, the theoretical study of steady, standing shock formation in accretion discs around non-rotating BHs has suffered from two general limitations. Firstly, the shock solutions were obtained either on a case by case basis, or, even when successful attempts were made to provide a more complete analysis, the boundary of the parameter space responsible for shock formation was obtained only for global variation of the total specific energy $\mathcal{E}$ (or accretion rate $\dot{M}$) and specific angular momentum λ of the flow, and not for variations of the polytropic constant γ of the flow; rather accretion was always considered to be ultra-relativistic [2] which may *not* always be a realistic assumption. As γ is expected to

[2]By the term 'ultra-relativistic' and 'purely non-relativistic' we mean a flow with $\gamma = \frac{4}{3}$ and $\gamma = \frac{5}{3}$ respectively, according to the terminology used in Frank et. al. 1992.

have great influence on the radiative properties of the flow in general, we think that ignoring the explicit dependence of shock solutions on γ limits claims of generality. Secondly, except for YK, all available so called global shock solutions have been discussed only in the context of one particular type of BH potential, namely, the Paczyński & Wiita (1980) potential (Φ_1 hereafter). Along with the Φ_1, recent studies (Das & Sarkar 2001; hereafter DS, and references therein) enhance the importance of also considering three other pseudo-Schwarzschild BH potentials, one (Φ_2 hereafter) proposed by Nowak & Wagoner (1991), and two others (Φ_3 and Φ_4 hereafter) due to Artemova, Björnsson & Novikov (Artemova, Björnsson & Novikov 1996, ABN hereafter), in mimicking the complete general relativistic space-time for accretion around a Schwarzschild black hole. Hence we believe that being restricted to only one specific pseudo-Schwarzschild BH potential does not guarantee the claimed 'global' nature of so called global shock solutions present in the literature, rather one must study the transonic disc structure as well as shock formation in *all* available BH potentials to firmly assert the ubiquity of shock formation in multi-transonic accretion disc around a Schwarzschild BH. In this context, it is to be mentioned here that YK deserves special importance because the shock solution due to YK appears to be the only work available in the literature which provides the complete general relativistic description of shock formation *exclusively* for a non-rotating BH. Nevertheless, this work deals only with isothermal accretion but one understands that global isothermality in BH accretion is difficult to achieve for realistic flows and more general kind of BH accretion is expected to be governed by polytropic equation of state. Also YK does not provide the global parameter space dependence of shock solutions. A few authors claim to provide the full general relativistic shock solutions for Schwarzschild BHs as a limiting case of their results obtained in Kerr geometry (Chakrabarti 1996a,b; Lu, Yu, Yuan & Young 1997, LY3 hereafter). In doing so, a number of assumptions were made, some of which, however, may not appear to be fully convincing. For example, either the disc was supposed to be in conical equilibrium (LY3), which should not be the case in reality because the realistic accretion flow should be in vertical equilibrium (Chakrabarti 1996 and references therein); some results valid for isothermal accretion were directly applied to study the polytropic accretion in an ad-hoc manner (Chakrabarti 1996a), or some of the Newtonian approximations were not very convincingly combined with complete general relativistic equations (Chakrabarti 1996b) which does not strengthen their claim for a full general relativistic treatment of shock formation. Hence it is fair to say that although literature on general relativistic hydrodynamic BH accretion is well enriched by a number of important works (The following is an incomplete list of relevant papers on the subject: Novikov & Thorne 1973, NT hereafter, Bardeen & Petterson 1975, Abramowicz, Jaroszynski & Sikora 1978, Lu 1985,1986, Karas & Mucha 1993, Björnsson 1995, Riffert & Herold 1995, Ipser 1996, Pariev 1996, Peitz & Appl 1997, Bao, Wiita & Hadrava 1998, Gammie & Popham 1998, Gammie 1999), no well accepted complete general relativistic global shock solution exclusively obtained for a hydrodynamic accretion disc around a Schwarzschild BH has yet appeared in the literature.

Motivated by above mentioned limitations encountered by previous works in this field, the major aim of our work presented in this paper is to provide a generalized formalism which is expected to handle the formation of steady, standing Rankine- Hugoniot shock (RHS) in multi-transonic hydrodynamic BH accretion flow and to identify which region of parameter space (spanned by every important accretion parameter, namely, $\mathcal{E}$, λ and γ), will be responsible for such shock formation for *all* available pseudo- Schawarzschild BH potentials. We would also like to compare the properties of multi transonic accretion in these BH potentials with complete general relativistic BH accretion as long as the issue of shock formation is concerned.

Hereafter, we will define the Schwarzschild radius r_g as

$$r_g = \frac{2GM_{BH}}{c^2}$$

(where M_{BH} is the mass of the black hole, G is universal gravitational constant) so that the marginally bound circular orbit r_b and the last stable circular orbit r_s take the values $2r_g$ and $3r_g$ respectively for a typical Schwarzschild black hole. Also, total mechanical energy per unit mass on r_s (sometimes called 'efficiency' e) may be computed as -0.057 for this case. Also, we will use a simplified geometric unit throughout this paper where radial distance r is scaled in units of r_g, radial dynamical velocity u and polytropic sound speed a of the flow is scaled in units of c (the velocity of light in vacuum), mass m is scaled in units of M_{BH} and all other derived quantities would be scaled accordingly. Also, for simplicity,we will use $G = c = 1$. In next section, we will briefly describe a few important features of the four different pseudo-Schwarzschild 'effective' BH potentials used in this work. In §3, we will show how we formulate and solve the equations governing multi-transonic BH accretion in these potentials which may have shocks. In §4, we will study multi-transonic BH accretion using the full general relativistic frame work and will try to argue (in an indirect, but self consistant manner) which potential is expected to be the closest approximation of actual general relativistic solutions for which regions of parameter space spanned by $\mathcal{E}$, λ and γ, as long as one concentrates only on shocked flows. Finally in §5 we will draw our conclusion by highlighting some of the possible important impacts of study of shock formation on related fields.

2. Properties of four pseudo- Schwarzschild BH potentials

Rigorous investigation of the complete general relativistic multi-transonic BH accretion disc structure is extremely complicated. At the same time it is understood that, as relativistic effects play an important role in the regions close to the accreting black hole (where most of the gravitational potential energy is released), purely Newtonian gravitational potential (in the form $\Phi_N = -\frac{1}{r}$) cannot be a realistic choice to describe transonic black hole accretion in general. To compromise between the ease of handling of a Newtonian description of gravity and the realistic situations described by complicated general relativistic calculations, a series of 'modified' Newtonian potentials have been introduced to describe the general relativistic effects that are most important for accretion disk structure around Schwarzschild and Kerr black holes (see ABN for further discussion). Introduction of such potentials allows one to investigate the complicated physical processes taking place in disc accretion in a semi-Newtonian framework by avoiding pure general relativistic calculations so that most of the features of spacetime around a compact object are retained and some crucial properties of the analogous relativistic solutions of disc structure could be reproduced with high accuracy. Hence, those potentials might be designated as 'pseudo-Kerr' or 'pseudo-Schwarzschild' potentials, depending on whether they are used to mimic the space time around a rapidly rotating or non rotating/ slowly rotating (Kerr parameter $a \sim 0$) black holes respectively. Below we describe four such pseudo Schwarzschild potentials on which we will concentrate in this paper. It is important to note that as long as one is not interested in astrophysical processes extremely close (within $1-2\ r_g$) to a black hole horizon, one may safely use the following BH potentials to study accretion on to a Schwarzschild black hole with the advantage that use of these potentials would simplify calculations by allowing one to use some basic features of flat geometry (additivity of energy or de-coupling of various energy components, i.e., thermal ($\frac{a^2}{\gamma-1}$), Kinetic ($\frac{u^2}{2}$) or gravitational (Φ) etc., see subsequent discussions) which is not possible for calculations in a purely Schawarzschild metric (see §4). Also, one can study more complex many body problems such as accretion from an ensemble of companions or overall efficiency of accretion onto an ensemble of black holes in a galaxy or for studying numerical hydrodynamic accretion flows around a black hole etc. as simply as can be done in a Newtonian framework, but with far better accuracy. So we believe that a comparative study of multi-transonic accretion flow as well as shock formation using all these potentials might be quite useful in understanding some important features of various shock related astrophysical phenomena, at least until one can have a complete and self-consistent theory of complete general relativistic shock formation exclusively for a Schwarzschild BH. However, one should be careful in using these potentials because none of these potentials discussed here are 'exact' in a sense that they are not directly derivable from the Einstein equations. These potentials could only be used to obtain more accurate correction terms over and above the pure Newtonian results and any 'radically' new results obtained using these potentials should be cross-checked very carefully with the exact general relativistic theory.

Paczyński and Wiita (1980) proposed a pseudo-schwarzschild potential of the form

$$\Phi_1 = -\frac{1}{2(r-1)} \tag{1a}$$

which accurately reproduces the positions of r_s and r_b and gives the value of efficiency to be -0.0625 which is in closest agreement with the value obtained in full general relativistic calculations. Also the Keplarian distribution of angular momentum obtained using this potential is exactly same as that obtained in pure Schwarzschild geometry. It is worth mentioning here that this potential was first introduced to study a thick accretion disc with super Eddington Luminosity. Also, it is interesting to note that although it had been thought of in terms of disc accretion, Φ_1 is spherically symmetric with a scale shift of r_g.
To analyze the normal modes of accoustic oscillations within a thin accretion disc around a compact object (slowly rotating black hole or weakly magnetized neutron star), Nowak and Wagoner (1991) approximated some of the dominant relativistic effects of the accreting black hole (slowly rotating or nonrotating) via a modified Newtonian potential of the form

$$\Phi_2 = -\frac{1}{2r}\left[1 - \frac{3}{2r} + 12\left(\frac{1}{2r}\right)^2\right] \tag{1b}$$

Φ_2 has correct form of r_s as in the Schwarzschild case but is unable to reproduce the value of r_b. This potential has the correct general relativistic value of the angular velocity Ω_s at r_s. Also it reproduces the radial epicyclic frequency κ (for $r > r_s$) close to its value obtained from general relativistic calculations, and among all BH potentials, Φ_2 provides the best approximation for Ω_s and κ. However, this potential gives the value of efficiency as -0.064 which is larger than that produced by Φ_1, hence the disc spectrum computed using Φ_2 would be more luminous compared to a disc structure studied using Φ_1.
Considering the fact that the free-fall acceleration plays a very crucial role in Newtonian gravity, ABN proposed two different BH potentials to study disc accretion around a non-rotating black hole. The first potential proposed by them produces exactly the same value of the free-fall acceleration of a test particle at a given value of r as is obtained for a test particle at rest with respect to the Schwarzschild reference frame, and is given by

$$\Phi_3 = -1 + \left(1 - \frac{1}{r}\right)^{\frac{1}{2}} \tag{1c}$$

The second one gives the value of the free fall acceleration that is equal to the value of the covariant component of the three dimensional free-fall acceleration vector of a test particle that is at rest in the Schwarzschild reference frame and is given by

$$\Phi_4 = \frac{1}{2} ln\left(1 - \frac{1}{r}\right) \tag{1d}$$

Efficiencies produced by Φ_3 and Φ_4 are -0.081 and -0.078 respectively.The magnitude of efficiency produced by Φ_3 being maximum,calculation of disc structure using Φ_3 will give the maximum amount of energy dissipation and the corresponding spectrum would be the most luminous one. Hereafter we will refer to all these four potentials by Φ_i in general, where $\{i = 1, 2, 3, 4\}$ would correspond to Φ_1 (eqn. 1(a)), Φ_2 (eqn. 1(b)), Φ_3 (eqn. 1(c)) and Φ_4 (eqn. 1(d)) respectively. One should notice that while all other Φ_is have singularity at $r = r_g$, only Φ_2 has a singularity at $r = 0$. It can be shown that for $r > 2r_g$, while Φ_2 is flatter compared to purely Newtonian potential Φ_N, all other Φ_is are steeper to Φ_N.
At any radial distance r measured from the accretor, one can define the effective potential $\Phi_i^{eff}(r)$ to be the summation of the gravitational potential and the centrifugal potential for matter accreting under the influence of ith pseudo potential. $\Phi_i^{eff}(r)$ can be expressed as:

$$\Phi_i^{eff}(r) = \Phi_i(r) + \frac{\lambda^2(r)}{2r^2} \tag{2a}$$

where $\lambda(r)$ is the non-constant distance dependent specific angular momentum of accreting material. One then easily shows that $\lambda(r)$ may have an upper limit:

$$\lambda_i^{up}(r) = r^{\frac{3}{2}}\sqrt{\Phi_i'(r)} \tag{2b}$$

where $\Phi_i'(r)$ represents the derivative of $\Phi_i(r)$ with respect to r. For weakly viscous or inviscid flow, angular momentum can be taken as a constant parameter (λ) and eqn. (2a) can be approximated as:

$$\Phi_i^{eff}(r) = \Phi_i(r) + \frac{\lambda^2}{2r^2} \tag{2c}$$

For general relativistic treatment of accretion, the effective potential can *not* be decoupled in to its gravitational and centrifugal components. For a Schwarzschild metric of the following form:

$$ds^2 = g_{\mu\nu}dx^\mu dx^\nu$$
$$= -\left(1-\frac{1}{r}\right)dt^2 + \left(1-\frac{1}{r}\right)^{-1}dr^2 + r^2\left(d\theta^2 + sin^2\theta d\phi^2\right)$$

the world line of the accreting fluid is timelike, and the four velocity of the fluid satisfies the normalization condition:

$$u_\mu u^\mu = -1$$

where $u^\mu(u_\mu)$ is the contra(co)-variant four velocity of the fluid. The angular velocity Ω of the fluid can be computed as

$$\Omega = \frac{u^\phi}{u^t} = -\frac{\lambda g_{tt}}{g_{\phi\phi}} = \frac{\lambda\,(r-1)}{2r^3}$$

where $\lambda = -\frac{u_\phi}{u_t}$ is the specific angular momentum which is conserved for fluid dynamics as well as for particle dynamics for invicid flow. The general relativistic effective potential $\Phi^{eff}_{GR}(r)$ (*excluding* the rest mass) experienced by the fluid accreting on to a Schwarzschild BH can be expressed as:

$$\Phi^{eff}_{GR}(r) = r\sqrt{\frac{r-1}{r^3-\lambda^2(1+r)}} - 1 \tag{2d}$$

One can understand that the effective potentials in general relativity cannot be obtained by linearly combining its gravitational and rotational contributions because various energies in general relativity are combined together to produce non-linearly coupled new terms.
In Fig 1, we plot $\Phi^{eff}_i(r)$ (obtained from eq. (2c)) and $\Phi^{eff}_{GR}(r)$ as a function of r in logarithmic scale. The value of λ is taken to be 2 in units of $2GM/c$. Φ^{eff} curves for different Φ_i are marked exclusively in the figure and the curve marked by $\mathbf{G^R}$ represents the variation of $\Phi^{eff}_{GR}(r)$ with r. One can observe that $\Phi^{eff}_1(r)$ is in excellent agreement with $\Phi^{eff}_{GR}(r)$, only for a very small value of r ($r \rightarrow r_g$), Φ^{eff}_1 starts deviating from $\Phi^{eff}_{GR}(r)$ and this deviation keeps increasing as matter approaches closer and closer to the event horizon. All other $\Phi^{eff}_i(r)$s approaches to $\Phi^{eff}_{GR}(r)$ at a radial distance (measured from the BH) considerably larger compared to the case for $\Phi^{eff}_1(r)$. If one defines $\Delta^{eff}_i(r)$ to be the measure of the deviation of $\Phi^{eff}_i(r)$ with $\Phi^{eff}_{GR}(r)$ at any point r,

$$\Delta^{eff}_i(r) = \Phi^{eff}_i(r) - \Phi^{eff}_{GR}(r)$$

One observes that $\Delta^{eff}_i(r)$ is always negative for $\Phi^{eff}_1(r)$, but for other $\Phi^{eff}_i(r)$, it normally remains positive for low values of λ but may become negative for a very high value of λ. If $|\Delta^{eff}_i(r)|$ be the modules or the absolute value of $\Delta^{eff}_i(r)$, one can also see that, although only for a very small range of radial distance very close to the event horizon, $\Delta^{eff}_3(r)$ is maximum, for the whole range of distance scale while Φ_1 is the best approximation of general relativistic space time, Φ_2 is the worst approximation and Φ_4 and Φ_3 are the second and the third best approximation as long as the total effective potential experienced by the accreting fluid is concerned. It can be shown that $|\Delta^{eff}_i(r)|$ nonlinearly anti-correlates with λ. The reason behind this is understandable. As λ decreases, rotational mass as well as its coupling term with gravitational mass decreases for general relativistic accretion material while for accretion in any Φ_i, centrifugal force becomes weak and gravity dominates; hence deviation from general relativistic case will be more prominent because general relativity is basically a manifestation of strong gravity close to the compact objects.
From the figure it is clear that for $\Phi^{eff}_{GR}(r)$ as well as for all $\Phi^{eff}_i(r)$s, a peak appears close to the horizon. The height of these peaks may roughly be considered as the measure of the strength of the centrifugal barrier encountered by the accreting material for respective cases. The deleberate use of the word 'roughly' instead of 'exactly' is due to the fact that

here we are dealing with fluid accretion, and unlike particle dynamics, the distance at which the strength of the centrifugal barrier is maximum, is located further away from the peak of the effective potential because here the total pressure contains the contribution due to fluid or 'ram' pressure also. Naturally the peak height for $\Phi_{GR}^{eff}(r)$ as well as for $\Phi_i^{eff}(r)$s increases with increase of λ and the location of this barrier moves away from the BH with higher values of angular momentum. If the specific angular momentum of accreting material lies between the marginally bound and marginally stable value, an accretion disc is formed. For invicid or weakly viscous flow, the higher will be the value of λ, the higher will be the strength of the centrifugal barrier and the more will be the amount of radial velocity or the thermal energy that the accreting material must have to begin with so that it can be made to accrete on to the BH. In this connection it is important to observe from the figure that accretion under $\Phi_1(r)$ will encounter a centrifugal barrier farthest away from the BH compared to other Φ_is. For accretion under all Φ_is except Φ_1,the strength of centrifugal barrier at a particular distance will be more compared to its value for full general relativistic accretion.

3. Multi-transonic flow in various BH potentials and shock formation

Following standerd literature, we consider a thin, rotating, axisymmetric, invicid steady flow in hydrostatic equilibrium in transverse direction. The assumption of hydrostatic equilibrium is justified for a thin flow because for such flows, the infall time scale is expected to exceed the local sound crossing time scale in the direction transverse to the flow. The flow is also assumed to posses considerably large radial velocity which makes the flow 'advective'. The complete solutions of such a system require the dimensionless equations for conserved specific energy $\mathcal{E}$ and angular momentum λ of the accreting material, the mass conservation equations supplied by the transonic conditions at the sonic points and the Rankine Hugoniot conditions at the shock. The local half-thickness, $h_i(r)$ of the disc for any $\Phi_i(r)$ can be obtained by balancing the gravitational force by pressure gradient and can be expressed as:

$$h_i(r) = a\sqrt{r/\left(\gamma\Phi_i'\right)}$$

For a non-viscous flow obeying the polytropic equation of state $p = K\rho^\gamma$ (K is a measure of the specific entropy of the flow), integration of radial momentum equation:

$$u\frac{du}{dr} + \frac{1}{\rho}\frac{dP}{dr} + \frac{d}{dr}\left(\Phi_i^{eff}(r)\right) = 0$$

leads to the following energy conservation equation in steady state:

$$\mathcal{E} = \frac{1}{2}u_e^2 + \frac{a_e^2}{\gamma - 1} + \frac{\lambda^2}{2r^2} + \Phi_i = 0; \qquad (3a)$$

and the continuity equation:

$$\frac{d}{dr}\left[u\rho r h_i(r)\right]=0$$

can be integrated to obtain the barion number conservation equation:

$$\dot{M}_{in}=\sqrt{\frac{1}{\gamma}}u_e a_e \rho_e r^{\frac{3}{2}}\left(\Phi_i'\right)^{-\frac{1}{2}}. \tag{3b}$$

Following C89, one can define the entropy accretion rate $\dot{\mathcal{M}}=\dot{M}_{in}K^{\left(\frac{1}{\gamma-1}\right)}\gamma^{\left(\frac{1}{\gamma-1}\right)}$ which undergoes a discontinuous transition at the shock location r_{sh} where local turbulence generates entropy to increase $\dot{\mathcal{M}}$ for post-shock flows. For our purpose, explicit expression for $\dot{\mathcal{M}}$ can be obtained as:

$$\dot{\mathcal{M}}=\sqrt{\frac{1}{\gamma}}u_e a_e^{\left(\frac{\gamma+1}{\gamma-1}\right)} r^{\frac{3}{2}}\left(\Phi_i'\right)^{-\frac{1}{2}}. \tag{3c}$$

In Eqs. (3a-3c), the subscript e indicates the values measured on the equatorial plane of the disc; however, we will drop e hereafter if no confusion arises in doing so. One can simultaneously solve Eqs. (3a - 3c) for any particular $\Phi_i(r)$ and for a particular set of values of $\{\mathcal{E},\lambda,\gamma\}$. Hereafter we will use the notation $[\mathcal{P}_i]$ for a set of values of $\{\mathcal{E},\lambda,\gamma\}$ for any particular Φ_i.

For a particular value of $[\mathcal{P}_i]$, it is now quite straight-forward to derive the space gradient of dynamical flow velocity $\left(\frac{du}{dr}\right)_i$ for flow in any particular ith BH potential $\Phi_i(r)$:

$$\left(\frac{du}{dr}\right)_i=\frac{\left(\frac{\lambda^2}{r^3}+\Phi_i'(r)\right)-\frac{a^2}{\gamma+1}\left(\frac{3}{r}+\frac{\Phi_i''(r)}{\Phi_i'(r)}\right)}{u-\frac{2a^2}{u(\gamma+1)}} \tag{4a}$$

where Φ_i'' represents the derivative of Φ_i'. Since the flow is assumed to be smooth everywhere, if the denominator of eqn. 4(a) vanishes at any radial distance r, the numerator must also vanish there to maintain the continuity of the flow. One therefore arrives at the so called 'sonic point (alternately, the 'critical point') conditions' by simultaneously making the numerator and denominator of eqn. 4(a) equal zero. The sonic point conditions can be expressed as:

$$a_s^i=\sqrt{\frac{1+\gamma}{2}}u_s^i=\left[\frac{\Phi_i'(r)+\gamma\Phi_i'(r)}{r^2}\left(\frac{\lambda^2+r^3\Phi_i'(r)}{3\Phi_i'(r)+r\Phi_i''(r)}\right)\right]_s \tag{4b}$$

where the subscript s indicates that the quantities are to be measured at the sonic point(s). For a fixed $[\mathcal{P}_i]$, one can solve the following polynomial of r to obtain the sonic point(s) of the flow:

$$\mathcal{E}-\left(\frac{\lambda^2}{2r^2}+\Phi_i\right)_s-\frac{2\gamma}{\gamma^2-1}\left[\frac{\Phi_i'(r)+\gamma\Phi_i'(r)}{r^2}\left(\frac{\lambda^2+r^3\Phi_i'(r)}{3\Phi_i'(r)+r\Phi_i''(r)}\right)\right]_s=0. \tag{4c}$$

Similarly, the value of $\left(\frac{du}{dr}\right)_i$ at its corresponding sonic point(s) can be obtained by solving the following equation:

$$\frac{4\gamma}{\gamma+1}\left(\frac{du}{dr}\right)^2_{s,i}-2u_s\left(\frac{\gamma-1}{\gamma+1}\right)\left(\frac{3}{r}+\frac{\Phi_i^{''}(r)}{\Phi_i^{'}(r)}\right)_s\left(\frac{du}{dr}\right)_{s,i}$$
$$+a_s^2\left[\frac{\Phi_i^{'''}(r)}{\Phi_i^{'}(r)}-\frac{2\gamma}{\left(1+\gamma\right)^2}\left(\frac{\Phi_i^{''}(r)}{\Phi_i^{'}(r)}\right)^2+\frac{6\left(\gamma-1\right)}{\gamma(\gamma+1)^2}\left(\frac{\Phi_i^{''}(r)}{\Phi_i^{'}(r)}\right)-\frac{6\left(2\gamma-1\right)}{\gamma^2(\gamma+1)^2}\right]_s$$
$$+\Phi_i^{''}\Big|_s-\frac{3\lambda^2}{r_s^4}=0 \qquad (4d)$$

Where the subscript (s,i) indicates that the corresponding quantities for any ith potential is being measured at its corresponding sonic point(s) and $\Phi_i^{'''}(r)=\frac{d^3\Phi_i(r)}{dr^3}$.

For *all* Φ_i's, we find a significant region of parameter space spanned by $[\mathcal{P}_i]$ which allows the multiplicity of sonic points for accretion as well as for wind where two real physical inner and outer (with respect to the BH location) X type sonic points r_{in} and r_{out} encompass one O type unphysical middle sonic point r_{mid} in between. For a particular Φ_i, if $\mathcal{A}_i\left[\mathcal{P}_i\right]$ denotes the universal set representing the entire parameter space covering all values of $[\mathcal{P}_i]$, and if $\mathcal{B}_i\left[\mathcal{P}_i\right]$ represents one particular subset of $\mathcal{A}_i\left[\mathcal{P}_i\right]$ which contains only the particular values of $[\mathcal{P}_i]$ for which the above mentioned three sonic points are obtained, then $\mathcal{B}_i\left[\mathcal{P}_i\right]$ can further be decomposed into two subsets $\mathcal{C}_i\left[\mathcal{P}_i\right]$ and $\mathcal{D}_i\left[\mathcal{P}_i\right]$ such that:

$$\mathcal{C}_i\left[\mathcal{P}_i\right]\ \subseteq\ \mathcal{B}_i\left[\mathcal{P}_i\right]\ \underline{\text{only for}}\ \dot{\mathcal{M}}\left(r_{in}\right)>\dot{\mathcal{M}}\left(r_{out}\right),$$

and

$$\mathcal{D}_i\left[\mathcal{P}_i\right]\ \subseteq\ \mathcal{B}_i\left[\mathcal{P}_i\right]\ \underline{\text{only for}}\ \dot{\mathcal{M}}\left(r_{in}\right)<\dot{\mathcal{M}}\left(r_{out}\right),$$

then for $[\mathcal{P}_i]\in\mathcal{C}_i\left[\mathcal{P}_i\right]$, we get multi-transonic *accretion* and for $[\mathcal{P}_i]\in\mathcal{D}_i\left[\mathcal{P}_i\right]$ one obtains multi-transonic *wind*. In Fig. 2. we plot

$$\left(\mathcal{E}_i,\lambda_i\right)\in\left[\mathcal{P}_i\right]\in\mathcal{C}_i\left[\mathcal{P}_i\right]\ \subseteq\ \mathcal{B}_i\left[\mathcal{P}_i\right]\ \underline{\text{and}}\ \left(\mathcal{E}_i,\lambda_i\right)\in\left[\mathcal{P}_i\right]\in\mathcal{D}_i\left[\mathcal{P}_i\right]\ \subseteq\ \mathcal{B}_i\left[\mathcal{P}_i\right]$$

for all $\Phi_i(r)$s (marked in the figure) when $\gamma=4/3$. While the specific energy $\mathcal{E}$ is plotted along the Y axis, the specific angular momentum λ is plotted along X axis. For $\Phi_1(r)$, the shaded region **PQR** represents the parameter space spanned by $\mathcal{E}$ and λ for which three sonic points will form in *accretion* (**PQR**$\equiv\mathcal{C}_1\left[\mathcal{P}_1\right]$) while the wedge shaped un-shaded region **PSR** represents the parameter space for which three sonic points are formed in *wind* (**PSR**$\equiv\mathcal{D}_1\left[\mathcal{P}_1\right]$). Similar kind of parameter space division is shown for other $\Phi_i(r)$s as well. A careful analysis of Fig. 2 reveals the fact that, at least for ultra-relativistic flow, *no* region of parameter space common to all $\Phi_i(r)$ is found for which $[\mathcal{P}_i]\in\mathcal{C}_i\left[\mathcal{P}_i\right]$ or $[\mathcal{P}_i]\in\mathcal{D}_i\left[\mathcal{P}_i\right]$. However, significant region of parameter space is obtained for which $[\mathcal{P}_i]\in\mathcal{C}_i\left[\mathcal{P}_i\right]$ or $[\mathcal{P}_i]\in$

$\mathcal{D}_i\,[\mathcal{P}_i]$ for $\Phi_2(r)$ and $\Phi_3(r)$ and a very small region of such common zone in the parameter space is obtained (only for extremely low values of the energy and angular momentum of the acceting matter) for $\Phi_2(r)$, $\Phi_3(r)$ and $\Phi_4(r)$. As the flow approaches to its purely non-relativistic limit, i.e., as we make $\gamma \longrightarrow 5/3$, tendency for such mutual overlap of parameter space for $\Phi_2(r)$, $\Phi_3(r)$ and $\Phi_4(r)$ increases. Nevertheless, Φ_1 still remains 'untouchable' by $\Phi_2(r)$ and $\Phi_3(r)$; only a particular region of parameter space (fairly low energy accretion with intermediate value of angular momentum) is commonly shared by $\Phi_4(r)$ and $\Phi_1(r)$.
One also observe that if $\mathcal{E}_i^{max}$ and λ_i^{max} are the maximum available energy and angular momentum of the flow for any $\Phi_i(r)$ for which $[\mathcal{P}_i] \in \mathcal{C}_i\,[\mathcal{P}_i]$ or $[\mathcal{P}_i] \in \mathcal{D}_i\,[\mathcal{P}_i]$, one can write:

$$\mathcal{E}_3^{max} \;>\; \mathcal{E}_4^{max} \;>\; \mathcal{E}_1^{max} \;>\; \mathcal{E}_2^{max}$$

and

$$\lambda_1^{max} \;>\; \lambda_4^{max} \;>\; \lambda_2^{max} \;>\; \lambda_3^{max}$$

The above trend remains unaltered as $\gamma \longrightarrow 5/3$ and we observe that both $\mathcal{E}_i^{max}$ and λ_i^{max} non-linearly anti-correlates with γ.
If shock forms in accretion (in this work we will not study the shock formation in wind), then $[\mathcal{P}_i]$s responsible for shock formation must be somewhere from the region for which $[\mathcal{P}_i] \in \mathcal{C}_i\,[\mathcal{P}_i]$, though not all $[\mathcal{P}_i] \in \mathcal{C}_i\,[\mathcal{P}_i]$ will allow shock transition. Using Eqs. (3a - 3c), we combine the three standard Rankine-Hugoniot conditions (Landau & Lifshitz 1959) for vertically integrated pressure and density (see Matsumoto et al. 1984) to derive the following relation which is valid *only* at the shock location:

$$(1-\gamma)\left(\frac{\rho_{-}\dot{\mathcal{M}}_{-}}{\dot{M}}\right)^{log_{\Gamma}^{1-\Theta}} \mathcal{E}_{(ki+th)} - \Theta(1+\Theta-R_{comp})^{-1} + (1+\Theta)^{-1} = 0, \qquad (5)$$

where $\mathcal{E}_{(ki+th)}$ is the total specific thermal plus mechanical energy of the accreting fluid: $\mathcal{E}_{(ki+th)} = \left[\mathcal{E} - \left(\frac{\lambda^2}{2r^2} + \Phi_i\right)\right]$, R_{comp} and β are the density compression and entropy enhancement ratio respectively, defined as $R_{comp} = (\rho_{+}/\rho_{-})$ and $\beta = \left(\dot{\mathcal{M}}_{+}/\dot{\mathcal{M}}_{-}\right)$ respectively; $\Theta = 1 - \Gamma^{(1-\gamma)}$ and $\Gamma = \beta R_{comp}$, "+" and "-" refer to the post- and pre-shock quantities. The shock strength $\mathcal{S}_i$ (ratio of the pre- to post-shock Mach number of the flow) can be calculated as:

$$\mathcal{S}_i = R_{comp}\,(1+\Theta)\,. \qquad (6)$$

Eqs. (5) and (6) cannot be solved analytically because they are non-linearly coupled. However, we have been able to simultaneously solve Eqs. (3 - 6) using iterative numerical techniques. We have developed an efficient numerical code which takes $[\mathcal{P}_i]$ and Φ_i as its input and can calculate r_{sh} along with any sonic or shock quantity as a function of $[\mathcal{P}_i]$. It is to be noted that like the references cited in §1, we also obtain multiplicity in the shock location. Following C89, we perform the local stability analysis and find that only one r_{sh} which forms in between r_{out} and r_{mid} is stable for *all* Φ_i.

If $[\mathcal{P}_i] \in \mathcal{F}_i\,[\mathcal{P}_i] \;\subseteq\; \mathcal{C}_i\,[\mathcal{P}_i]$ represents the region of parameter space for which multi-transonic supersonic flows is expected to encounter a RHS at r_{sh}, where they become hotter, shock compressed and subsonic and will again become supersonic only after passing through r_{in} before ultimately crossing the event horizon, then one can also define $[\mathcal{P}_i] \in \mathcal{G}_i\,[\mathcal{P}_i]$ which is complement of $\mathcal{F}_i\,[\mathcal{P}_i]$ related to $\mathcal{C}_i\,[\mathcal{P}_i]$ so that for:

$$\left\{ \mathcal{G}_i\,[\mathcal{P}_i] \,\middle|\, [\mathcal{P}_i] \in \mathcal{C}_i\,[\mathcal{P}_i] \text{ and } [\mathcal{P}_i] \notin \mathcal{F}_i\,[\mathcal{P}_i] \right\},$$

the shock location becomes imaginary in $\mathcal{G}_i\,[\mathcal{P}_i]$, hence no stable RHS forms in that region; rather the shock keeps oscillating back and forth. We anticipate that $\mathcal{G}_i\,[\mathcal{P}_i]$ is also an important zone which might be responsible for the Quasi-Periodic Oscillation (QPO) of the BH candidates (see §5).

Figure 3 demonstrates few typical flow topologies of the integral curves of motion for ultra-relativistic ($\gamma = 4/3$) shocked flows in various Φ_i's (indicated in the figure). While the distance from the event horizon of the central BH (scaled in the units of r_g and plotted in logarithmic scale) is plotted along the X axis, the local Mach number of the flow is plotted along the Y axis. One can easily obtain such a set of figures for any γ (and $[\mathcal{P}_i]$) which allow shock formation. For all figures, **ABCD** represents the transonic accretion passing through the outer sonic point r_{out} (marked as **B**) if a shock would not form. However, as $\dot{\mathcal{M}}$ of the flow is higher at the inner sonic point r_{in} compared to $\dot{\mathcal{M}}$ at r_{out}, the flow must encounter a shock at **C** (the vertical line **CE** marked by an arrowhead represents the shock transition), becomes subsonic and jumps on the branch **EF**, which ultimately hits the event horizon supersonically after it passes through the inner sonic point r_{in}, which is marked on **EF** by the small circle with a dot at the center. An "$*$" in the figure indicates the location of the middle sonic point r_{mid}. The corresponding values of r_{in}, r_{mid}, r_{out}, the shock location r_{sh}, and shock strength S_i are indicated at the top of each figure, while the corresponding values of the total specific energy $\mathcal{E}$ and angular momentum λ for which the solutions are obtained, are indicated inside each figure. **GBH** represents the 'self-wind' of the flow, which, in the course of its motion *away* from the BH to infinity, becomes supersonic after passing through r_{out} at **B**. Collectively, **ABCEF** represents the real physical shocked accretion which connects infinity with the event horizon. The overall scheme for obtaining the above mentioned integral curves is as follows:

First we compute r_{in}, r_{mid} and r_{out} by solving eq. (4c). Then we obtain the dynamical velocity gradient of the flow at sonic points by solving eq. (4d). For a chosen $\dot{M}_{in}$ (scaled in the units of the Eddington rate $\dot{M}_{Edd}$), we then compute the local dynamical flow velocity

$u(r)$, the local polytropic sound speed $a(r)$, the local radial Mach number $M(r)$, the local fluid density $\rho(r)$ and any other related dynamical or thermodynamic quantities by solving the eq. (4a-4d) from the outer sonic point using fourth order Runge-Kutta method. We start integrating from r_{out} in two different directions. Along **BH**, we only solve for $u(r)$, $a(r)$ and $M(r)$ because shock does not form in subsonic flows. However, integration along **BCD** involves a different procedure. Along **BCD**, not only we compute $u(r)$, $a(r)$ and $M(r)$, but also, at *every* integration step (with as small a step size as possible), we keep checking whether eq. (5) is being satisfied at that point. To do so, at each and every point, we start with a suitable initial guess value of R_{comp} and $\mathcal{S}_i$ and performs millions of iteration to check whether for any set of $[R_{comp}, \mathcal{S}_i]$, eq. (5) is satisfied at that point and whether for such $[R_{comp}, \mathcal{S}_i]$, the value of β obtained from eq. (5) becomes exactly equal to $\frac{\dot{\mathcal{M}}(r_{in})}{\dot{\mathcal{M}}(r_{out})}$; in other words, whether the entropy generated at that point (if any) becomes exactly equal to the difference between the entropies at the inner and the outer sonic points respectively. If such conditions are satisfied at some particular point (point **C** in the figure), we argue that the shock forms at that point and we can calculate any pre- and the post-shock dynamical and thermodynamic quantities at the shock location r_{sh} (i.e., at **C**). Once a shock is formed, the flow jumps from its supersonic branch **BCD** to its subsonic branch **EG**. We again start calculating $u(r)$, $a(r)$ and $M(r)$ and any other related flow quantities by solving eq. (4a) using fourth order Runge-Kutta method (with the help of eq. (3a-3c) and eq. (4d)), but this time from the *inner* sonic point r_{in} of the flow.

In Figure 4, we present the $\mathcal{F}_i\,[\mathcal{P}_i]$s for all four Φ_i's ($\Phi_1 \rightarrow$(a), $\Phi_2 \rightarrow$ (b), $\Phi_3 \rightarrow$ (c), and $\Phi_4 \rightarrow$ (d)). The specific energy $\mathcal{E}$, specific angular momentum λ and the polytropic index γ of the flow are plotted along the Z, Y and X axis respectively. Each surface for a particular $\Phi_i(r)$ is drawn for a particular value of γ. While the first surfaces (which have the maximum surface areas) on the $(\mathcal{E} - \gamma)$ plane represent ultra-relativistic accretion ($\gamma = 4/3$), successive surfaces are also shown for higher values of γ, taking a regular interval of $\Delta\gamma = 0.025$. It is observed that as the flow approaches to its purely non-relativistic limit, the area of the $(\mathcal{E} - \gamma)$ surfaces responsible for shock formation starts shrinking. We find that the shock location correlates with λ. This is obvious because the higher will be the flow angular momentum, the greater will be the rotational energy content of the flow and the higher will be the strength of the centrifugal barrier (which is responsible to break the incoming flow by forming a shock) as well as the further will be the location of such barrier from the event horizon. However, r_{sh} anti-correlates with $\mathcal{E}$ and γ. which means that for same $\mathcal{E}$ and λ, shock in purely non-relativistic flow will form closer to the event horizon compared to the ultra-relativistic flow. We also observe that the shock strength $\mathcal{S}_i$ non-linearly anti-correlates with the shock location r_{sh}, which indicates that the closer the shock forms to the BH, the higher is the strength $\mathcal{S}_i$ and the entropy enhancement ratio β. The ultra-relativistic flows are supposed to produce the strongest shocks. The reason behind this is also easy to understand; the closer the shock forms to the event horizon, the higher will be the available gravitational potential energy to be released and the higher will be the radial advective velocity required to have a more vigorous shock jump. Compared to Φ_2 and Φ_3, Φ_1 and Φ_4 allow wider spans of γ as well as λ for shock formation. If $\mathcal{E}_{max}$, λ_{max} and γ_{max} represents the maximum values of the corresponding parameters for which shock formation is possible, we obtain $\mathcal{E}_{max}(\Phi_3) > \mathcal{E}_{max}(\Phi_4) > \mathcal{E}_{max}(\Phi_1) > \mathcal{E}_{max}(\Phi_2)$, $\lambda_{max}(\Phi_1) > \lambda_{max}(\Phi_4) > \lambda_{max}(\Phi_3) > \lambda_{max}(\Phi_2)$ and $\gamma_{max}(\Phi_4) > \gamma_{max}(\Phi_1) > \gamma_{max}(\Phi_3) > \gamma_{max}(\Phi_2)$, respectively. Also we observe that as more and more the flow approaches its purely non-relativistic limit, shock may form for less and less angular momentum. For some $\Phi_i(r)$s, even a very small amount of angular momentum ($\lambda < 1$) allows shock formation, which indicates that for purely non-relativistic accretion, shock formation may take place even for quasi-spherical flow.

4. General Relativistic multi-transonic accretion

Following the arguments provided by NT and Chakrabarti 1996a, we derive the expressions for the conserved total specific energy $\mathcal{E}'$ (which *includes* the rest mass energy) and the entropy accretion rate $\dot{\mathcal{M}}$ as:

$$\mathcal{E}' = \frac{\gamma(\gamma-1)}{\gamma-(1+a^2)}\sqrt{\frac{r-1}{1-u^2}}\left[r^3+\lambda^2(1-r)\right]^{-\frac{1}{2}} \tag{7a}$$

and

$$\dot{\mathcal{M}} = 5.657ur^{1.25}\sqrt{\frac{r-1}{1-u^2}}\left[\frac{a^2(\gamma-1)}{\gamma-(1+a^2)}\right]^{\frac{\gamma+1}{2(\gamma-1)}}\left[r^3+\lambda^2(1-\gamma)\right]^{0.25} \tag{7b}$$

One can see from eq. (7a) that the total specific energy in this case, can *not* be decoupled into various linearly additive contributions of separate physical origin (i.e., kinetic, thermal, rotational or gravitational) as it could be done for flows in any pseudo-potential.
Following the procedure outlined in previous section, one can derive the dynamical flow velocity gradient for general relativistic accretion flow as:

$$\left(\frac{du}{dr}\right) = \left(\frac{\frac{1}{2r}\left[\frac{2r^3-\lambda^2}{r^3+\lambda^2(1-\gamma)}\right] - \frac{2r-1}{2r(r-1)} - \frac{2a^2}{\gamma+1}\left[\frac{5-7r}{4r(r-1)}+\frac{\lambda^2-3r^2}{4[r^3+\lambda^2(1-r)]}\right]}{\left[\frac{2a^2}{u(u^2-1)(\gamma+1)}+\frac{u}{1-u^2}\right]}\right) \tag{8a}$$

from which the sonic point conditions comes out to be:

$$u_s = \sqrt{\frac{2}{\gamma+1}}a_s = \sqrt{\frac{\gamma+1}{2}\left[\frac{\frac{1}{2r}\left[\frac{2r^3-\lambda^2}{r^3+\lambda^2(1-\gamma)}\right]-\frac{2r-1}{2r(r-1)}}{\frac{5-7r}{4r(r-1)}+\frac{\lambda^2-3r^2}{4[r^3+\lambda^2(1-r)]}}\right]_s} \tag{8b}$$

The sonic point(s) could be computed by solving the following equation:

$$\mathcal{E}'^2\left[r_s^3+\lambda^2\left(1-r_s\right)\right]-\frac{r_s-1}{1-\mathbf{\Psi}\left(\mathbf{r_s},\lambda\right)}\left[\frac{\gamma\left(\gamma-1\right)}{\gamma-\eta\left(\mathbf{r_s},\lambda\right)}\right]^2=0 \tag{8c}$$

where

$$\eta\left(\mathbf{r_s},\lambda\right)=\left[1+\frac{\gamma+1}{2}\mathbf{\Psi}\left(\mathbf{r_s},\lambda\right)\right]$$

and

$$\mathbf{\Psi}\left(\mathbf{r_s},\lambda\right)=\left[\frac{\frac{1}{2r_s}\left[\frac{2r_s^3-\lambda^2}{r_s^3+\lambda^2(1-\gamma)}\right]-\frac{2r_s-1}{2r_s(r_s-1)}}{\frac{5-7r_s}{4r(r_s-1)}+\frac{\lambda^2-3r_s^2}{4[r_s^3+\lambda^2(1-r_s)]}}\right]$$

The dynamical flow velocity gradient at the sonic point(s) can be obtained by solving the following equation:

$$\frac{2\left(2\gamma-3a_s^2\right)}{\left(\gamma+1\right)\left(u_s^2-1\right)^2}\left(\frac{du}{dr}\right)_s^2+4\xi\left(\mathbf{r_s},\lambda\right)\left[\frac{\gamma-\left(1+a_s^2\right)}{u_s^2-1}\right]\left(\frac{du}{dr}\right)_s$$
$$+\frac{2}{\gamma+1}a_s^2\xi\left(\mathbf{r_s},\lambda\right)\left[2\xi\left(\mathbf{r_s},\lambda\right)\left[\frac{\gamma-\left(1+a_s^2\right)}{\gamma+1}\right]-\frac{2r_s-1}{r_s\left(r_s-1\right)}-\frac{3r_s^2-\lambda^2}{r_s^3+\lambda^2\left(1-r_s\right)}\right.$$
$$\left.+\frac{40r_s^3-24r_s^2-\lambda^2\left(16r_s-13\right)}{10r_s^4-8r_s^3-\lambda^2\left(8r_s^2-13r_s+5\right)}\right]=0 \tag{8d}$$

where

$$\xi\left(\mathbf{r_s},\lambda\right)=\left[\frac{5-7r}{4r\left(r-1\right)}+\frac{\lambda^2-3r^2}{4\left[r^3+\lambda^2\left(1-r\right)\right]}\right]$$

We solve eq. (8c) and find that like flows in various $\Phi_i(r)$s, here also a significant region of parameter space allows the multiplicity of sonic points for accretion as well as for wind where one O type unphysical middle sonic point is flanked in between two X type real physical sonic points r_{in} and r_{out} respectively. In Fig. 5 we show the regions of parameter space for which multi-transonic flow is obtained for both accretion and wind. The dimensionless conserved total specific energy $\mathcal{E}$ (*excluding* the rest mass energy) is plotted along the Y axis whereas the specific angular momentum λ is plotted along the X axis. In region bounded by **PQR** and marked by $\mathcal{A}$, three sonic points are formed in accretion and in region bounded by **PRS** and marked by $\mathcal{W}$, three sonic points are formed in wind. While the figure is drawn for ultra-relativistic flows, the corresponding regions of parameter space can be obtained for any γ. If $\mathcal{E}_{max}$ be the maximum value of the energy and if λ_{max} and λ_{min} be the maximum and minimum values of the angular momentum respectively, for which three sonic points are formed in accretion for any particular γ, we observe that $[\mathcal{E}_{max}, \lambda_{max}, \lambda_{min}]$ non-linearly anti-correlates with γ. In other words, as the flow approaches its purely non-relativistic limit, the area of the region involved in formation of multi-transonic accretion decreases to a lower value.

In Fig. 6, we show the integral curves of motion for general relativistic accretion of ultra-relativistic polytropic fluid. For a particular set of $[\mathcal{E}, \lambda, \gamma]$ shown in the figure, **ABCD** represents the accretion passing through the outer sonic point r_{out} (marked in the figure by **B**) location of which can be found by solving eq. (8c). **EBI** represents the self-wind. Flow along **EFGH** passes through the inner sonic point r_{in} (marked in the figure by **F**) and encompasses a middle sonic point r_{mid} location of which is shown in the figure using a "$*$". Like Fig. 3, here also we obtain the complete solution topology by integrating eq. (8a) (with the help of eq. (7a-7b) and eq. (8c)) using fourth order Runge-Kutta method.

If Σ and Π be the shock compression and the entropy enhancement ratio (at the shock location) for this case ($\Sigma = \frac{M_-}{M_+}$, $\Pi = \frac{\dot{\mathcal{M}}_+}{\dot{\mathcal{M}}_-}$), one can show that the following equation will be satisfied when shock forms:

$$\Pi\Sigma^{\frac{1}{1-\gamma}} \left(\frac{T_-}{T_+}\right)^{\frac{\gamma}{\gamma-1}} \left(\frac{1-u_-^2}{1-u_+^2}\right)^{\frac{1}{4}\left(\frac{3-\gamma}{\gamma-1}\right)} = 1 \tag{9}$$

where $T(-/+)$ and $u(-/+)$ are the pre-/post-shock temperature and dynamical velocities of the flow respectively. However, it is our limitation in this paper that we have not been able to formulate or solve any equation which can be used to calculate the shock location in general relativistic accretion onto Schwarzschild BHs. Nevertheless, if shock forms in such flow (which is, of course, expected), it is obvious that the set of $(\mathcal{E}, \lambda)$ responsible for shock formation *must* belong to the region **PQR** ($\equiv [\mathcal{P}_{GR}] \in \mathcal{C}_{GR}[\mathcal{P}_{GR}]$, see §3) of Fig. 5 because shock will form *only* in multi-transonic accretion. The above argument is useful to compare accretion flows in various $\Phi_i(r)$s with general relativistic accretion (at least as long as the question of of shock formation in multi-transonic flow is concerned) in the following way:

Suppose for ultra-relativistic flows, we take the region of parameter space $[\mathcal{P}_i] \in \mathcal{F}_i[\mathcal{P}_i]$ for any $\Phi_i(r)$ used in this paper (see Fig. 4), and then superpose that region with **PQR** of Fig. 5 and study which $\Phi_i(r)$ provides the maximum overlap between $[\mathcal{P}_i] \in \mathcal{F}_i[\mathcal{P}_i]$ and $[\mathcal{P}_{GR}] \in \mathcal{C}_{GR}[\mathcal{P}_{GR}]$. That particular BH potential is then considered to be the most efficient pseudo-potential in approximating the general relativistic, multi-transonic, shocked BH accretion. However, such an 'efficiency test' is not entirely unambiguous because as we are yet to figure out the exact $[\mathcal{P}_{GR}] \in \mathcal{F}_{GR}[\mathcal{P}_{GR}]$, there may be some possibility that for any $\Phi_i(r)$, though $[\mathcal{P}_i] \in \mathcal{F}_i[\mathcal{P}_i]$ will overlap with $[\mathcal{P}_{GR}] \in \mathcal{C}_{GR}[\mathcal{P}_{GR}]$, but instead of falling onto $[\mathcal{P}_{GR}] \in \mathcal{F}_{GR}[\mathcal{P}_{GR}]$, it will rather overlap with $[\mathcal{P}_{GR}] \in \mathcal{G}_{GR}[\mathcal{P}_{GR}]$ because the exact boundary between $[\mathcal{P}_{GR}] \in \mathcal{F}_{GR}[\mathcal{P}_{GR}]$ and $[\mathcal{P}_{GR}] \in \mathcal{G}_{GR}[\mathcal{P}_{GR}]$ could not be explored in our work. Nevertheless, we believe that still our arguments for the 'efficiency test' is of some use, at least until one can find out the exact shock formation zone for general relativistic flow.

In Fig. 7, we superpose the Fig. 5 on $[\mathcal{P}_i] \in \mathcal{F}_i[\mathcal{P}_i]$ for all different $\Phi(r)$s (marked in the figure) used in our work. Unlike other $[\mathcal{P}_i] \in \mathcal{F}_i\,[\mathcal{P}_i]$s, $[\mathcal{P}_3] \in \mathcal{F}_3\,[\mathcal{P}_3]$ are drawn using long-dashed lines to show its overlap with $[\mathcal{P}_2] \in \mathcal{F}_2\,[\mathcal{P}_2]$. The figure is drawn for ultra-relativistic flow but can also be drawn for other γs as well. We observe that while $[\mathcal{P}_1] \in \mathcal{F}_1\,[\mathcal{P}_1]$ has *excellent* overlap (except at very high energy) with $[\mathcal{P}_{GR}] \in \mathcal{C}_{GR}\,[\mathcal{P}_{GR}]$, *no other* $[\mathcal{P}_i] \in \mathcal{F}_i\,[\mathcal{P}_i]$s have any overlap with it. This leads to the conclusion that at least for ultra-relativistic flow, not only $\Phi_1(r)$ is a very good approximation, rather it is the *only* BH potential to approximate for the general relativistic multi-transonic shocked flow. However, as the flow approaches its purely non-relativistic limit, we observe that the area of the ovarlaping zone for $\Phi_1(r)$ decreases with higher γ and $[\mathcal{P}_1] \in \mathcal{F}_1\,[\mathcal{P}_1]$ is pushed back to overlap rather with $[\mathcal{P}_{GR}] \in \mathcal{D}_{GR}\,[\mathcal{P}_{GR}]$; hence unlike ultra-relativistic accretion, $\Phi_1(r)$ may not be considered such a good approximation for purely non-relativistic flows. Also we find that a region of low energy - high angular momentum $[\mathcal{P}_4] \in \mathcal{F}_4\,[\mathcal{P}_4]$ starts overlapping with $[\mathcal{P}_{GR}] \in \mathcal{C}_{GR}\,[\mathcal{P}_{GR}]$. So for high γ flows, along with $\Phi_1(r)$, $\Phi_4(r)$ may also be considered as a plausible approximation for general relativistic accretion. Shocked flows in $\Phi_2(r)$ and $\Phi_3(r)$ *never* show any overlap with $[\mathcal{P}_{GR}] \in \mathcal{C}_{GR}\,[\mathcal{P}_{GR}]$ for any value of γ; hence these potentials may not be considered to mimick the general relativistic multi-transonic accretion flows.

5. Concluding Remarks

In this paper, we provide a generalized formalism which can formulate and solve the equations governing the advective, multi-transonic, hydrodynamic BH accretion in *all* available pseudo-Schwarzschild potentials, which may contain steady, standing, Rankine-Hugoniot kind of shocks. We have also formulated and solved the equations governing multi-transonic, complete general relativistic BH accretion and wind in Schwarzschild metric and compared our pseudo-Schwarzschild solutions with the general relativistic one. The main conclusions of this paper are the following:

(a) We observe that a significant region of parameter space (spanned by the conserved total specific energy $\mathcal{E}$, the specific angular momentum λ and the polytropic index γ of the flow) allows shock formation for *all* potentials, which leads to the strong conclusion that stable, standing RHS are inevitable ingredients in multi-transonic accretion disks around non-rotating BHs. The same kind of conclusion was drawn by previous works in this field (see §1) *only* for ultra-relativistic accretion in Paczyński & Wiita (1980) potential, whereas we make this conclusion more general by incorporating *all* available BH potentials to study BH accretion for *all* possible values of γ.

(b) As the shock forms at a particular radial distance, it is clear that self-similar solutions should *not* be invoked while studying real physical BH accretion and related phenomena.

(c) It is sometimes argued that a non-standing oscillating shock may modulate the disc spectrum in order to explain the dwarf novae outburst (Mausche, Raymond & Mattei 1995) or QPO (Hua, Kazanas & Titarchuk 1997). In this context, the region of parameter space, for which three sonic points are formed in accretion but still no steady, standing shock is found (see §3), can be considered as quite an important zone because $[\mathcal{P}_i] \in \mathcal{G}_i\,[\mathcal{P}_i]$ may provide the relevant parameters responsible for such physical processes.

(d) As long as the shock formation in ultra-relativistic black hole accretion is concerned, the Paczyński & Wiita (1980) potential $\Phi_1(r)$ is the *only* pseudo potential which can mimic the solutions of general relativistic accretion disc around non-rotating BHs in a very efficient way. However, in the purely non-relativistic limit ($\gamma \longrightarrow 5/3$), along with $\Phi_1(r)$, another BH potential $\Phi_4(r)$ proposed by ABN, is also observed to mimic the general relativistic solutions; at least for low energy - high angular momentum flows. However, it is interesting to note one important feature of the Paczyński & Wiita potential $\Phi_1(r)$; like spherically symmetric accretion (see DS), for accretion disc also, $\Phi_1(r)$ is observed to be in excellent agrement with solutions for ultra-relativistic flow in pure Schwarzschild metric, however, it starts loosing (albeight very slowly) its efficiency in mimicking full general relativistic solution with higher values of γ, i.e., as the flow reaches its purely non-relativistic limits; although the exact reason behind this is not quite clear to us.

Hot, dense and exo-entropic post-shock regions in advective accretion disks are used as a powerful tool in understanding the spectral properties of BH candidates (Shrader & Titarchuk 1998, and references therein) and in theoretically explaining a number of diverse phenomena, including millisecond variability in the X-ray emission from LMXBs and the generation mechanism for high frequency QPOs in general (Titarchuk, Lapidus & Muslimov 1998 and references therein), high energy emission from central engines of AGNs (Sivron, Caditz & Tsuruta 1996), formation of heavier elements in BH accretion discs via non-explosive nucleosynthesis (Mukhopadhyay & Chakrabarti 2000), formation and dynamics of accretion powered galactic and extragalactic jets, quiescent states of X-ray novae systems and outflow induced low luminosity of our galactic centre (Das 2001; Das & Chakrabarti 1999). A number of observational evidences are also present which are in close agreement with the theoretical predictions obtained from shocked accretion model (Rutledge et al. 1999; Muno, Morgan & Remillard 1999; Webb & Malkan 2000; Rao, Yadav & Paul 2000; Smith, Heindl & Swank 2001). Thus we believe that our present work may have far reaching consequences because of the following reasons:

1. Our generalized formalism assures that that our model is not just an artifact of a particular type of potential only and inclusion of every BH potential allows a substantially extended zone of parameter space allowing for the possibility of shock formation.

2. Of course there are possibilities that in future someone may come up with a pseudo-Schwarzschild potential better than $\Phi_1(r)$, which will be the best approximation for

complete general relativistic investigation of multi-transonic shocked flow. In such case, if one already formulates a generalized model for multi-transonic shocked accretion disc for any arbitrary $\Phi(r)$, exactly what we have done in this paper, then that generalized model will be able to readily accommodate that new $\Phi(r)$ without having any significant change in the fundamental structure of the formulation and solution scheme of the model and we need not have to worry about providing any new scheme exclusively valid only for that new potential, if any.

3. Even if someone can provide a completely satisfactory model for shock formation in full general relativistic (Schwarzschild) BH accretion, still the utility of this work may not be completely irrelevant. Rigorous investigation of some of the shock related phenomena is extremely difficult (if not completely impossible) to study using full general relativistic framework. Hence one is expected to always rely on these pseudo-potentials because of the ease of handling them. For example, it was shown that (see §4) the total energy of the general relativistic accretion flow can *not* be decoupled into its constituent contributions, whereas for any kind of pseudo-potential (see §2), all individual energy components are linear under addition. This provides enough freedom and ease to simply add any extra component in the expression for energy to introduce any new physics in the system (radiative forces or magnetic fields for example), which is certainly not possible while dealing with full general relativistic astrophysical flows around non-rotating BHs.

Thus, for above mentioned reasons, we believe that compared to all previous works based solely on ultra-relativistic accretion in Φ_1, our model is better equipped for handling various shock related phenomena.

It is noteworthy that the idea of shock formation in advective BH accretion is contested by some authors (Narayan, Kato & Honma 1997, and references therein). However, the fact that their claim against shock formation is, perhaps, inappropriate for many reasons, has been shown (Molteni, Gerardi & Valenza 2001) from energy considerations. One can understand that the problem of not finding shocks lies in the fact that non-shock ADAF models are, perhaps, unable to produce multi-transonic flows because only one inner sonic point close to the BH is explored by such works.

One can observe that flows characterized by $[\mathcal{P}_i] \in \mathcal{F}_i\,[\mathcal{P}_i]$ in our work may contain low intrinsic angular momentum for some cases (especially for purely non-relativistic flow in some of the BH potentials) However, such weakly rotating flows are expected to be allowed by nature for various real physical situations like detached binary systems fed by accretion from OB stellar winds (Illarionov & Sunyaev 1975; Liang & Nolan 1984), semi-detached low-mass non-magnetic binaries (Bisikalo et al. 1998) and supermassive BHs fed by accretion from slowly rotating central stellar clusters (Illarionov 1988; Ho 1999 and references therein).

Even twenty-eight years after the discovery of standard accretion disc theory (Shakura & Sunyaev 1973), exact modeling of viscous multi-transonic BH accretion, including proper heating and cooling mechanisms is still quite an arduous task, and we have not yet fully attempted this. However, our preliminary calculations show that the introduction of viscosity via a radius dependent power law distribution for angular momentum pushes the shock location closer to the BH; details of this work will be discussed elsewhere.

The author acknowledges discussions with Igor D. Novikov, A. R. Rao and Sandip K. Chakrabarti. His very special thanks goes to Paul J. Wiita for reading the manuscript extremely carefully and for providing a number of useful suggesstions. He is also thankful to Aveek Sarkar for checking some of the algebra. Finally, the hospitality provided by the Racah Institute of Physics, The Hebrew University of Jerusalem, Israel, is acknowledged, where a part of this paper was written.

REFERENCES

Abramowicz, M., Jaroszynski, M., & Sikora, M. 1978, A & A, 63, 221

Abramowicz, M., & Chakrabarti, S. K. 1990, ApJ, 350, 281

Artemova, I. V., Björnsson, G., & Novikov, I. D. 1996, ApJ, 461, 565 (ABN)

Babul, A., Ostriker, J. P., & Mészáros, P. 1989, ApJ, 347, 59

Bao,G., Wiita, P. J., & Hadrava, P. 1998, ApJ, 508,58

Bardeen, J. M., Petterson, J. A. 1975, ApJ, 195, L65

Bisikalo, A. A., Boyarchuk, V. M., Chechetkin, V. M., Kuznetsov, O. A., & Molteni, D. 1998, MNRAS, 300, 39

Bisnovatyi-Kogan, G. S., Zel'Dovich, Ya. B, & Syunyaev, R. A. 1971, Soviet Astronomy, 15, 17

Björnsson, G. 1995, ApJ, 441, 765

Blondin, J. M., & Ellison, D. C. 2001, ApJ, 560, 244

Blondin, J. M., & Konigl, A. 1987, ApJ, 323, 451

Caditz, D. M., & Tsuruta, S. 1998, ApJ, 501, 242

Chakrabarti, S. K. 1989, ApJ, 347, 365 (C89)

Chakrabarti, S. K. 1996, Physics Reports, 266, 229

Chakrabarti, S. K. 1996a, MNRAS, 283, 325

Chakrabarti, S. K. 1996b, ApJ, 471, 237

Chakrabarti, S. K., & Molteni, D. 1993, ApJ, 417, 671

Chang, K. M., & Ostriker, J. P. 1985, ApJ, 288, 428

Contopoulos, J., & Kazanas, D. 1995, ApJ, 441, 521

Das, T. K., 2001, Astrophys. & Space Sc., 276, 267

Das, T. K., 2001, A & A, 376, 697

Das, T. K., & Chakrabarti, S. K. 1999, Class. Quantum Grav, 16, 3879

Das, T. K., & Sarkar, A. 2001, A & A, 374, 1150 (DS)

Ferrari, A., Trussoni, E., Rosner, R., and Tsinganos, K. 1985, ApJ, 294, 397

Foglizzo, T. 2001, A & A, 368, 311

Foglizzo, T., & Tagger, M. 2000, A & A, 363, 174

Fukue, J. 1983, PASJ, 35, 355

Fukue, J. 1987, PASJ, 39, 309

Gammie, C., & Popham, R. 1998, ApJ, 498, 313

Gammie, C. 1999, ApJ, 522, L57

Guessoum, N., & Kazanas, D. 1999, ApJ, 512, 332

Hawley, J. F., Wilson, J. R., & Smarr, L. L. 1984, ApJ, 277, 296

Ho, L. C. 1999, in Observational Evidence For Black Holes in the Universe, ed. S. K. Chakrabarti (Dordrecht: Kluwer), 153

Hua, X. M., Kazanas, D., & Titarchuk, L. 1997, ApJ, 482, L57

Illarionov, A. F. 1988, Soviet Astron., 31, 618

Illarionov, A.F., & Sunyaev, R. A. 1975a, A & A, 39, 205

Ipser, J. 1996, ApJ, 458,508

Jones, F. C., & Ellison, D. C. 1991, Space Science Review, 58, 259

Karas, V., & Mucha, R. 1993, AmJph, 61,825

Kazanas, D., & Ellison, D. C. 1986, ApJ, 304, 178

Kovalenko I. G., & Eremin, M. A. 1998, MNRAS, 298, 861

Lai, D., & Goldreich, P. 2000, ApJ, 535, L402

Landau, L. D., & Lifshitz, E. D. 1959, Fluid Mechanics (New York: Pergamon)

Liang, E. P. T., & Nolan, P. L. 1984, Space Sci. Rev., 38, 353

Lu, J. F. 1985,A & A, 148, L176

Lu, J. F. 1986, GReGr, 18, L45

Lu, J. F., Yu, K. N., Yuan, F., & Young, E. C. M. 1997, A & A, 321, 665 (LY3)

Markoff, S., Melia, F., & Falcke, H. 1999, ApJ, 522, 870

Matsumoto, R., Kato. S., Fukue. J., & Okazaki. A. T. 1984, PASJ, 36, 71

Mauche, C. W., Raymond, J. C., & Mattei, J. A. 1995, ApJ, 446, 842

Mészáros, P. & Ostriker, J. P., 1983, ApJ, 273, L59

Molteni, D., Gerardi, G., & Valenza, M. A. 2001, ApJ, 551, L77

Mukhopadhyay, B. & Chakrabarti, S. K. 2000, A & A, 353, 1029

Muno, M. P., Morgan, E. H., & Remillard, R. A. 1999, Apj, 527, 321

Narayan, R., Kato, S., & Honma, F. 1997, ApJ, 476, 49

Novikov, I. D., & Thorne, K. S. 1973, in DeWitt C.,DeWitt B., eds, Black Holes. Gordon and Breach, New York (NT), p. 343

Nowak, A. M., & Wagoner, R. V. 1991, ApJ, 378, 656

Pariev, V. I. 1996, MNRAS, 283, 1264

Park, M. G. 1990, ApJ, 354, 64

Park, M. G. 1990a, ApJ, 354, 83

Paczyński, B., & Wiita, P. J. 1980, A & A, 88, 23

Peitz, J., Appl. S. 1997, MNRAS, 268, 681

Protheroe, R. J., & Kazanas, D. 1983, ApJ, 256, 620

Protheroe, R. J., & Szabo, A. P. 1992, Physical Review Letters, 69, 2885

Rao, A. R., Yadav, J. S., & Paul, B. 2000, ApJ, 544, 443

Riffert, H., & Herold, H. 1995, ApJ, 450, 508

Rutledge R E et al. 1999 ApJ Suppl. Ser. 124 265

Sawada, K., Matsuda, T., & Hachisu, I. 1986, MNRAS, 219, 75

Shakura, N. I., & Sunyaev, R. A. 1973, A & A, 24, 337

Shrader, C. R., & Titarchuk, L. G. 1998, ApJ, 499, L31

Sivron, R., Caditz, D., & Tsuruta, S. 1996, ApJ, 469, 542

Smith, D. M., Heindl, W. A., & Swank, J. H. 2001, To appear in ApJ (astro-ph/0103304).

Spruit, H. C. 1987, A & A, 184, 173

Titarchuk, L., Lapidus, I., & Muslimov, A. 1998, ApJ, 499, 315

Tóth, G., Keppens, R., & Botchev, M. A. 1998, A & A, 332. 1159

Webb, W., & Malkan, M. 2001, ApJ, 540, 652

Yang, R., & Kafatos, M. 1995, A & A, 295, 238 (YK)

This preprint was prepared with the AAS LaTeX macros v5.0.

Figure Captions

Fig. 1: Effective BH potentials for general relativistic ($\Phi_{BH}^{eff}(r)$) as well as for pseudo-general relativistic($\Phi_{i}^{eff}(r)$) accretion discs as a function of the distance (measured from the event horizon in units or r_g) plotted in logarithmic scale. The specific angular momentum is chosen to be 2 in geometric units. See text for details.

Fig. 2: Parameter space division for multi-transonic, ultra-relativistic accretion and wind in four different pseudo-Schwarzschild BH potentials, see text for details.

Fig. 3: Solution topologies for multi-transonic, ultra-relativistic ($\gamma = 4/3$) shocked flows in different BH potentials as indicated in the figure. See text for details.

Fig. 4: Region of parameter space responsible for shock formation ($\mathcal{F}_i\left[\mathcal{P}_i\right]$), for four different BH potentials Φ_1 (a), Φ_2 (b), Φ_3 (c), and Φ_4 (d). See text for details.

Fig. 5: Parameter space division for ultra-relativistic, multi-transonic, accretion and wind in general relativity.

Fig. 6: Integral curves of motion for ultra-relativistic, multi-transonic, black hole accretion and corresponding 'self-wind' in Schwarzschild metric. See text for details.

Fig. 7: Comparison of parameter space producing shocked multi-transonic accretion in various BH potentials, with parameter space representing multi-transonic black hole accretion and wind in general relativity. The figure is drawn for the ultra-relativistic flow, see text for details.

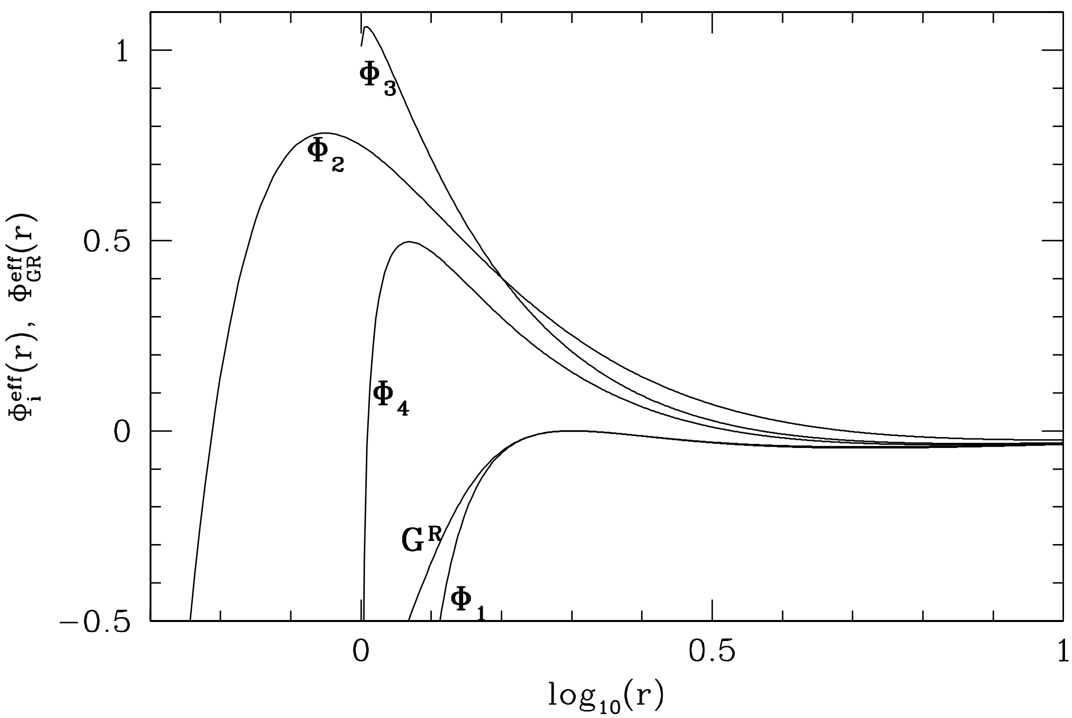
1
0.5
0
−0.5
0
0.5
1
log$_{10}$(r)
$\Phi_i^{eff}(r)$, $\Phi_{GR}^{eff}(r)$
Φ_3
Φ_2
Φ_4
G^R
Φ_1

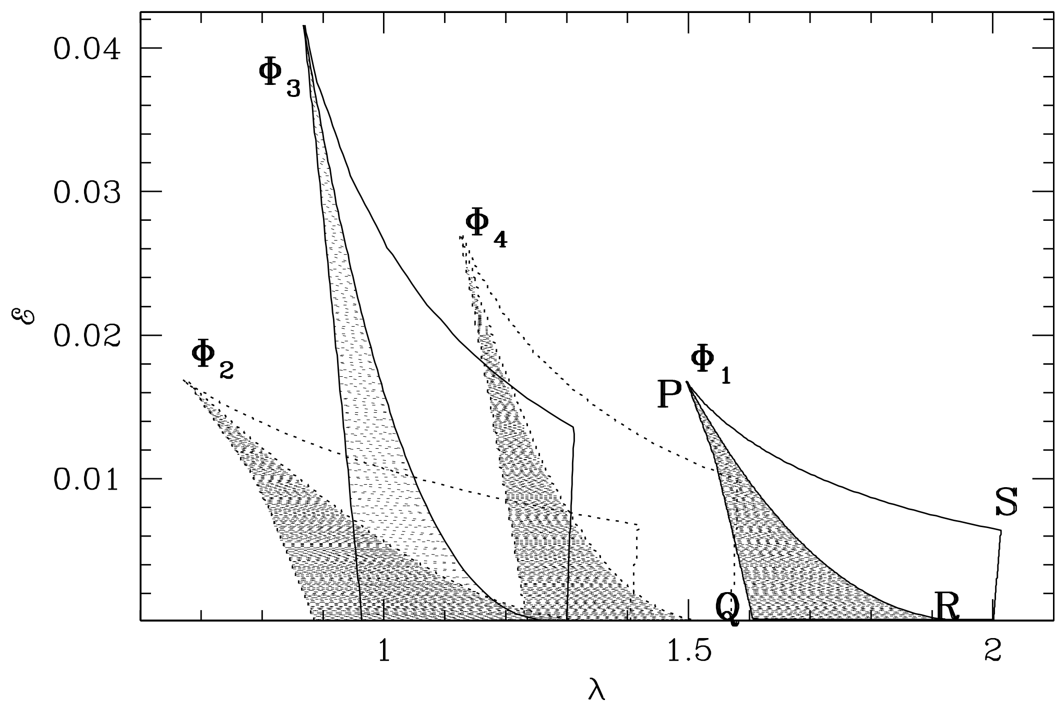
0.04
0.03
0.02
0.01
1
1.5
2
λ
ℰ
Φ3
Φ4
Φ2
Φ1
P
Q
R
S

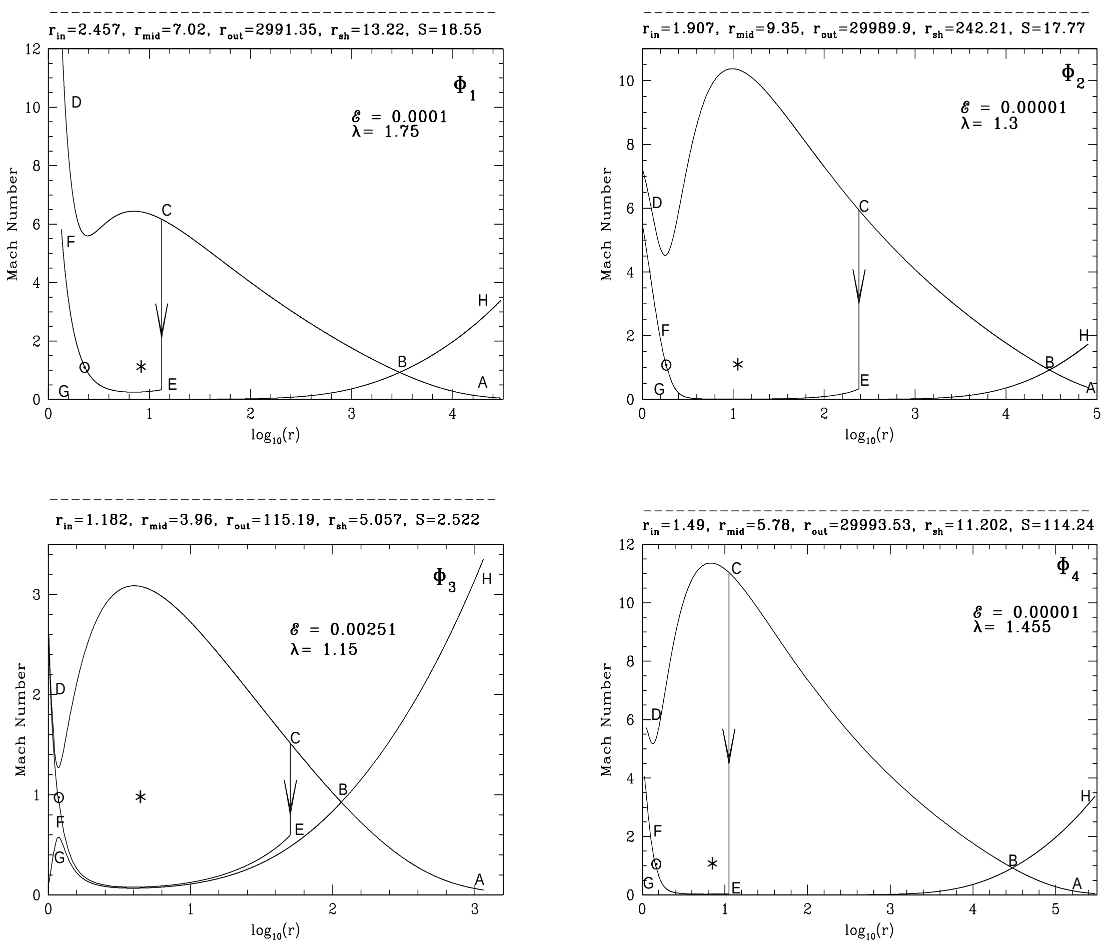

r_in=2.457, r_mid=7.02, r_out=2991.35, r_sh=13.22, S=18.55
Φ1
ℰ = 0.0001
λ= 1.75
r_in=1.907, r_mid=9.35, r_out=29989.9, r_sh=242.21, S=17.77
Φ2
ℰ = 0.00001
λ= 1.3
r_in=1.182, r_mid=3.96, r_out=115.19, r_sh=5.057, S=2.522
Φ3
ℰ = 0.00251
λ= 1.15
r_in=1.49, r_mid=5.78, r_out=29993.53, r_sh=11.202, S=114.24
Φ4
ℰ = 0.00001
λ= 1.455
Mach Number
log10(r)
A
B
C
D
E
F
G
H

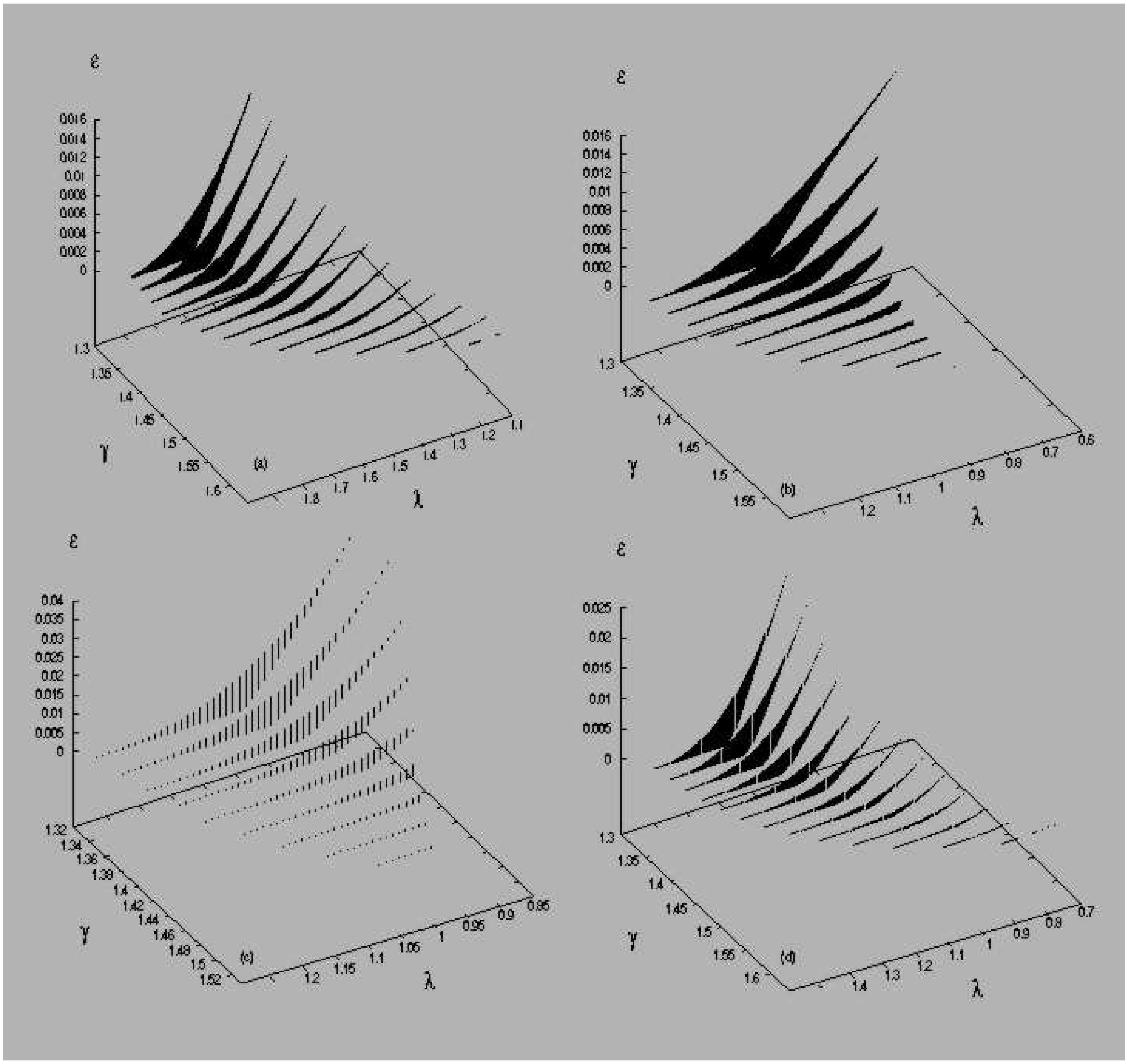
ε
γ
λ
(a)
(b)
(c)
(d)

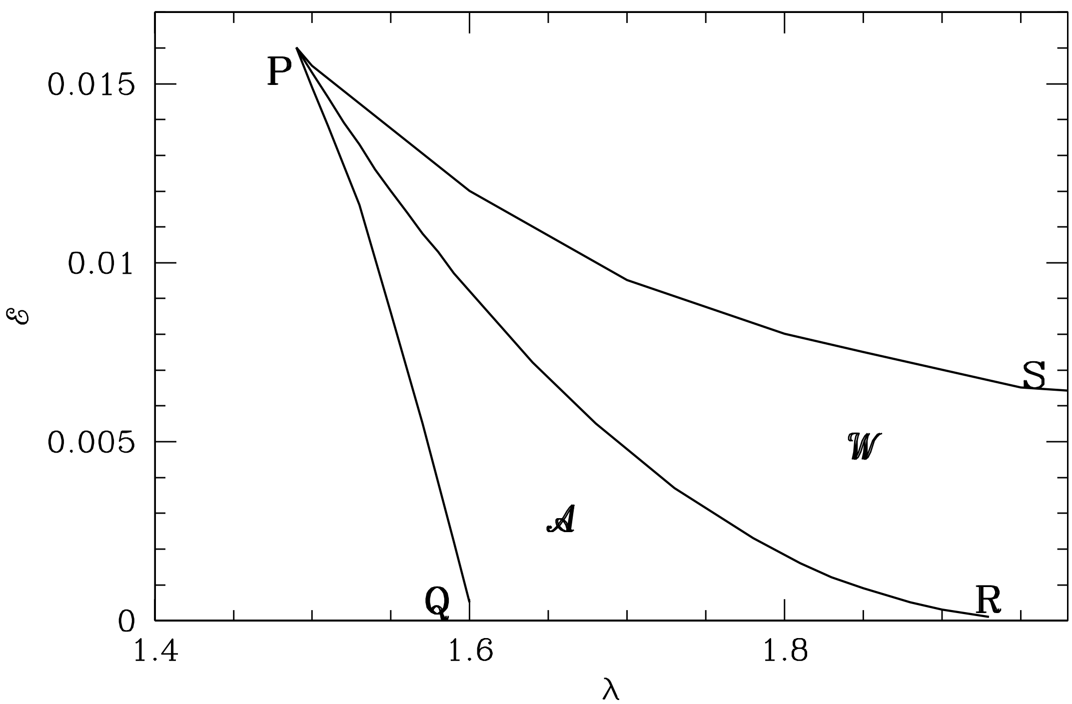
P
Q
R
S
$\mathscr{A}$
$\mathscr{W}$
0.015
0.01
0.005
0
1.4
1.6
1.8
$\mathscr{E}$
λ

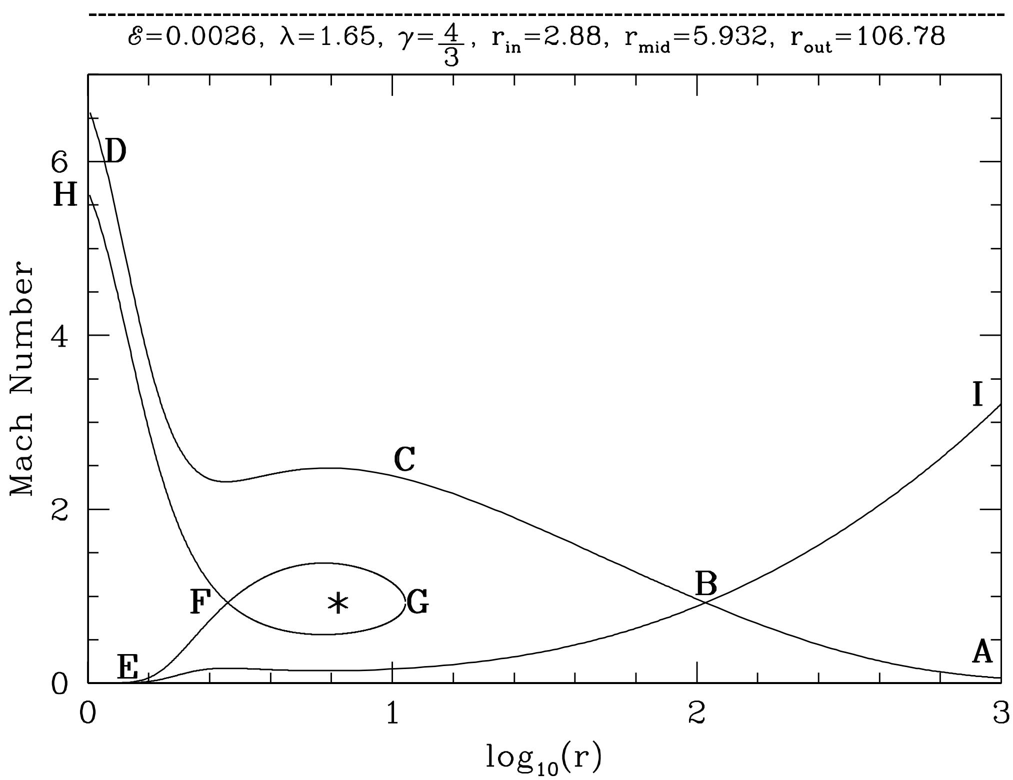

$\mathcal{E}$=0.0026, λ=1.65, γ=4/3, r_{in}=2.88, r_{mid}=5.932, r_{out}=106.78
Mach Number
$\log_{10}(r)$
A
B
C
D
E
F
G
H
I
0
1
2
3
0
2
4
6

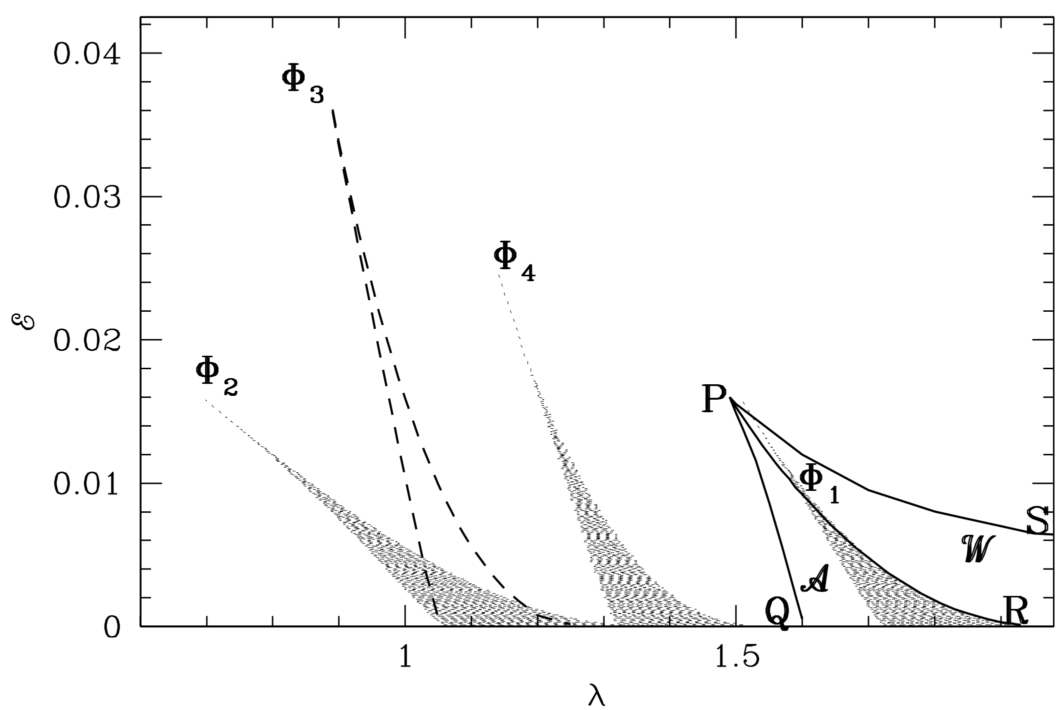
0.04
0.03
0.02
0.01
0
1
1.5
λ
ℰ
Φ_3
Φ_4
Φ_2
Φ_1
P
Q
R
S
𝒲
𝒜